

# Numerical Solution of a Casson Nanofluid flow and heat transfer analysis between Concentric Cylinders

Azad Hussain<sup>a,\*</sup>, Fouzia Javed<sup>a</sup>, Sohail Nadeem<sup>b</sup>

<sup>a</sup> University of Gujrat, Mathematics Department, Gujrat 50700

<sup>b</sup> Quaid-i-Azam University, Mathematics Department, Islamabad 44000, Pakistan.

## Abstract

The current investigation deals with heat transfer of a non-newtonian fluid between two concentric cylinders. To describe the behavior of non-Newtonian fluid casson fluid model is used because of its various useful applications. The governing partial differential equations suchlike continuity, momentum, energy, solute concentration and nano-particle fraction equations are transubstantiated into non-linear ordinary differential equations with the assistance of resemblance alteration. Then those are numerically solved by the very efficient shooting method. Additionally, influences of distinct involved parameters are interpreted graphically. It is adhered that the velocity field shows inclined behavior due to the increment in the values of the casson parameter, so long as enhancing the temperature.

**Keywords:** Heat transfer; Casson Nanofluid; Concentric cylinders; Numerical solution.

## 1. Introduction

The content matter of non-Newtonian fluid mechanics have much importance and of great interest in the area of research particularly technological and industrial problems. The cases in point to observe in real life are toothpaste, lava and ice, snow avalanches, tomato sauce and mayonnaise etc. The flowing attributes of non-Newtonian fluids are perfectly dissimilar from those of Newtonian fluids. We adhere that in the study of non-Newtonian problems, the order of governing equations is higher than the comparable Newtonian problems. Therefore, one needs the extra boundary conditions to obtain a unique solution. Such type of issue was interpreted by Malik et al. [1] during the investigation of third grade fluid flow between cylinders. Also the non-Newtonian fluids have more non-linear equations than the Newtonian fluids and it was not an easy task to obtain the numerical solution. In spite of all these hurdles, various researches [2–5] put efforts to find out the analytical solution for non-Newtonian fluids flow. Ramzan et al. [6] examined MHD non-Newtonian fluid flow over a vertically stretching sheet. Hussain et al. [7] observed Oldroyd 8-constant fluid flow between coaxial cylinders with inconsistent viscosity. Rizwan Ul Haq et al. [8] studied numerically the non-Newtonian fluid flow past over a stretchable surface. Many

models of non-Newtonian fluids have been suggested like Maxwell fluid model, Oldroyd-B fluid model, Viscoelastic fluids, Tangent hyperbolic fluid, Williamson fluid, Jeffrey fluid model, Power law fluid model etc. All these fluids express the non-linear behavior. M. Hameed et al. [9] observed the unsteady MHD non-Newtonian fluid flow on a porous plate.

The influence of magnetic field on Magnetohydrodynamic flow have very much significance and on large scale applications in many engineering problems. We may observe such kind of examples as glass manufacturing, purification of crude oil and geophysics. On account of wideranging multiple applications in engineering and industrial fields specifically from petroleum products the ancestry of crude oil, the investigation of non-newtonian fluids have captivated much attention of researchers [10–15]. The extension of classical cauchy stress on the account of non-Newtonian fluid laid down the foundation of exclusive theories [16–18].

For the classification of non-Newtonian fluids, Casson fluid has distinguishable attributes. In 1995, Casson presented this model for the viscoelastic fluids flow. By fuel engineers this model was cast off in the depiction of glutinous water mixture of insoluble matter. When only transitional shear rate data was attainable, it was improved for predicting high shear rate viscosities.

By power manufacturing, electronics and transportation the heating and cooling influences are required. For high energy devices these heating and cooling techniques are needed. It is very obvious that common fluids have limited

\*Corresponding author

Email address: azad.hussain@uog.edu.pk (Azad Hussain)

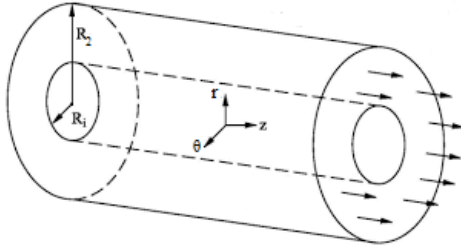


Figure 1: Geometry of the fluid flow

potential of heat transferring because of their low heat transferring ability. We observe that some metals have higher thermal conductivity, seems three or four times than common fluids. A substance is required which is made by combining these two fluids, behaving like having higher thermal conductivity metal as well as a fluid. Nanofluids are such kind of substances which are made by the suspension of nano particles into the common fluids. Common fluids are also called base fluids. A very small quantity of nanoparticles into the common fluids enlarges the thermal conductivity by 15-40%. The name of nanofluids was conceived by Choi very first time at Argonne National laboratory. It can improve the heat transfer rate as compared to pure liquids. For the better performance of thermal management system, nanofluids are used. For example, in engineering field like HVAC system, transportation, cooling devices and micromechanics. These fluids have wide range of applications in medical era too, as laser based surgery and cancer therapy. These are also employed for large scale cooling in aeroplanes and military systems. M. Sheikholeslami et al. [19] deliberated the consequences of heat transfer and thermal radiation on MHD nanofluid flow using two phase model. A. Zeeshan et al. [20] investigated MHD and heat transfer effects on CuO–water nanofluid flow. The influence of mixed convection on the flow of an Eyring-Powell nanofluid with stretching sheet was investigated by Malik et al. [21]. Rizwan Ul Haq et al. [22] investigated MHD squeezed nanofluid flow over a sensor surface.

An unbiased and central aim of the present investigation is to contemplate the unidimensional interpretation of the casson fluid model arrogant the two concentric cylinders. We eliminated the system of non-linear partial differential equations into the system of non-linear ordinary differential equations by amplification of resemblance alteration. To obtain the solution of coupled equations which are highly non-linear, are numerically attempted. We have acquired the solution of non-linear ordinary coupled differential equations by employing the shooting method along with R-K technique. Then with the assistance of graphs the fleshly behavior of each parameter is interpreted.

## 2. Formulation of the problem

We consider the steady state incompressible flow of a casson nanofluid bounded by two concentric cylinders. Following figure (Fig. 1) depicts the flow of fluid.

The governing equations for the present flow are given as,

$$\nabla \cdot V = 0, \quad (1)$$

$$\rho \left( \frac{\partial V}{\partial t} + V \cdot \nabla V \right) = -\nabla p + \mu \nabla^2 V, \quad (2)$$

$$k \nabla^2 T + (\rho c)_p [D_B \nabla \phi \cdot \nabla T + (\rho c)_f D_{TC} \nabla^2 C + \left( \frac{D_T}{T_\infty} \right) \nabla T \cdot \nabla T] = (\rho c)_f \left( \frac{\partial T}{\partial t} + V \cdot \nabla T \right), \quad (3)$$

$$\frac{\partial C}{\partial t} + V \cdot \nabla C = D_S \nabla^2 C + D_{CT} \nabla^2 T, \quad (4)$$

$$\frac{\partial \phi}{\partial t} + V \cdot \nabla \phi = D_B \nabla^2 \phi + \left( \frac{D_T}{T_f} \right) \nabla^2 T. \quad (5)$$

After solving eqs. (2) - (5), we have

$$\frac{dP}{dz} = \mu_\beta \left( 1 + \frac{1}{\beta} \right) \left[ \frac{d^2 v}{dr^2} + \frac{1}{r} \frac{dv}{dr} \right], \quad (6)$$

$$\frac{k}{(\rho c)_f} \left( \frac{d^2 T}{dr^2} \right) + \frac{k}{(\rho c)_f} \left( \frac{1}{r} \right) \left( \frac{dT}{dr} \right) + D_{TC} \left( \frac{d^2 C}{dr^2} \right) + D_{TC} \left( \frac{1}{r} \right) \left( \frac{dC}{dr} \right) + \frac{(\rho c)_p}{(\rho c)_f} \left( D_B \frac{d\phi}{dr} \cdot \frac{dT}{dr} \right) + \frac{(\rho c)_p}{(\rho c)_f} \left( \frac{D_T}{T_\infty} \right) \frac{dT}{dr} \cdot \frac{dT}{dr} = 0, \quad (7)$$

$$\left( \frac{d^2 C}{dr^2} + \frac{1}{r} \frac{dC}{dr} \right) + \frac{D_{CT}}{D_C} \frac{d^2 T}{dr^2} + \frac{D_{CT}}{D_C} \left( \frac{1}{r} \right) \left( \frac{dT}{dr} \right) = 0, \quad (8)$$

$$\left( \frac{d^2 \phi}{dr^2} + \frac{1}{r} \frac{d\phi}{dr} \right) + \frac{d^2 T}{dr^2} + \frac{D_T}{D_B T_f} \left( \frac{1}{r} \right) \left( \frac{dT}{dr} \right) = 0. \quad (9)$$

Where  $\mu_\beta$  is kinematic viscosity and  $\beta$  is casson fluid parameter.  $v$  is the velocity component along  $z$ -direction,  $\rho$  denotes density,  $p$  indicates fluid pressure,  $t$  denotes time,  $T$  depicts temperature and  $k$  denotes thermal conductivity.  $C$  describes solute concentration and  $\phi$  depicts nanoparticle fraction.

Boundary conditions are given as,

$$v(R_1) = v_1, v(R_2) = 0, T(R_1) = T_1, T(R_2) = 0, \quad (10)$$

$$C(R_1) = C_1, C(R_2) = 0, \phi(R_1) = \phi_1, \phi(R_2) = 0.$$

Here  $T_1$  is used for Temperature,  $C_1$  for solute concentration, and  $\phi_1$  for nano particle fraction at inner cylinder. Continuity equation is obviously satisfied for the given velocity profile.

## 3. Non-dimensional equations

We define,

$$\begin{aligned} r &= \frac{\bar{r}}{R_1}, v = \frac{\bar{v}}{v_1}, \theta = \frac{T}{T_1}, \phi = \frac{\bar{\phi}}{\phi_1}, \psi = \frac{\bar{C}}{C_1}, \\ P &= \frac{\frac{dP}{dz} R_1^2}{v_1 \mu_\beta}, \alpha = \frac{k}{(\rho c)_f}, \tau = \frac{(\rho c)_p}{(\rho c)_f}, C = \frac{D_{CT}}{D_C}, \\ A &= \frac{\tau \cdot T_1}{\alpha \cdot T_f} \cdot D_T, B = \frac{\tau}{\alpha} D_B \phi_1, \mu_c = \frac{\bar{\mu}}{\mu_1}. \end{aligned} \quad (11)$$

Where  $A$  is thermophoresis parameter,  $B$  is Brownian motion parameter,  $C$  is the Dufour-solutal Lewis number and  $F$  is the modified Dufour parameter. In the light of equatin 11, eqs. 6 - 9 occupy the shape (after dropping the bars),

$$P = (1 + \frac{1}{\beta}) \frac{d^2v}{dr^2} + \frac{1}{r} \frac{dv}{dr}, \tag{12}$$

$$\frac{d^2\theta}{dr^2} + \frac{1}{r} \frac{d\theta}{dr} + A(\frac{d\theta}{dr})^2 + B(\frac{d\theta}{dr})(\frac{d\phi}{dr}) + F(\frac{d^2\psi}{dr^2} + \frac{1}{r} \frac{d\psi}{dr}) = 0, \tag{13}$$

$$\frac{d^2\psi}{dr^2} + \frac{1}{r} \frac{d\psi}{dr} + C(\frac{d^2\theta}{dr^2} + \frac{1}{r} \frac{d\theta}{dr}) = 0, \tag{14}$$

$$\frac{d^2\phi}{dr^2} + \frac{1}{r} \frac{d\phi}{dr} + \frac{B}{A}(\frac{d^2\theta}{dr^2} + \frac{1}{r} \frac{d\theta}{dr}) = 0. \tag{15}$$

and related transformed boundary conditions are

$$v(1) = 1, v(2) = 0, \theta(1) = 1, \theta(2) = 0, \tag{16}$$

$$\psi(1) = 1, \psi(2) = 0, \phi(1) = 1, \phi(2) = 0.$$

#### 4. Solution of the problem

To get ordinary differential equations from the flow arising governing equations, the suitable similarity transformation is used. Shooting technique on eqs. 12-16 is used to find out the solution along with Runge Kutta method. The impact of different dimensionless quantities on velocity, concentration, nanoparticle fraction and temperature fields are interpreted with the assistance of graphs. Runge-Kutta method is one of the technique that is used to solve the intial value problems. First of all we transform momentum and energy equations in first order form i. e,

$$v'' = \frac{rP - v'}{r(1 + \frac{1}{\beta})}, \tag{17}$$

$$\theta'' = -\frac{\theta' + B\theta'\phi'r + Ar(\theta')^2 + Fr\psi'' + F\psi'}{r},$$

$$\psi'' = -\frac{\psi' + Cr\theta' + F\theta'}{r},$$

$$\phi'' = -\frac{\phi'A + B\theta''r + B\theta'}{r}.$$

Now, we define new variables that are applied to reduce the higher order ordinary differential equations into first order i. e,

$$v = r_1, v' = r_2, v'' = r_2', \tag{18}$$

$$\theta = r_3, \theta' = r_4, \theta'' = r_4',$$

$$\psi = r_5, \psi' = r_6, \psi'' = r_6',$$

$$\phi = r_7, \phi' = r_8, \phi'' = r_8'.$$

After putting the new variables, we get the new system of ordinary differential equations i. e,

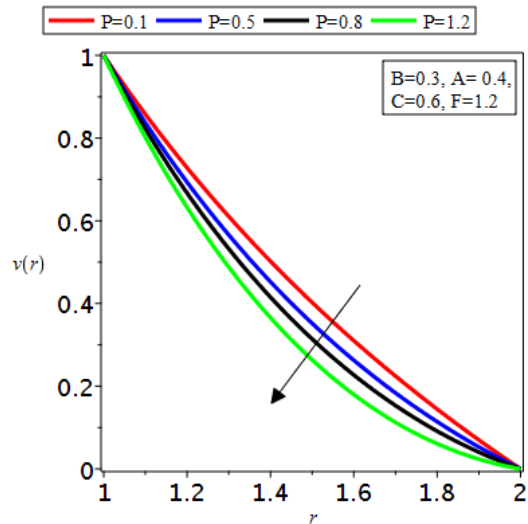


Figure 2: Influence of  $P$  on velocity profile

$$r_2' = \frac{rP - r_2}{r(1 + \frac{1}{\beta})}, \tag{19}$$

$$r_4' = -\frac{r_4 + Br_4r_8r + Ar(r_4)^2 + Fr r_6' + Fr_6}{r},$$

$$r_6' = -\frac{r_6 + Cr r_4' + Cr_4}{r},$$

$$r_8' = -\frac{r_8A + Br_4'r + Br_4}{r}.$$

In accordance with the boundary conditions,

$$r_1(1) = 1, r_1(2) = 0, \tag{20}$$

$$r_3(1) = 1, r_3(2) = 0,$$

$$r_5(1) = 1, r_5(2) = 0,$$

$$r_7(1) = 1, r_7(2) = 0.$$

#### 5. Results and Discussion

In the realm of graphical render, influences of pertinent parameters on temperature and velocity distributions are discussed concisely. Fig. 1 demonstrates the physical model of the concentric cylinders. The behavior of distinct parameters on different profiles are investigated. Fig. 2 depicts the effects of  $P$  on velocity distribution. The velocity distribution exhibits decreasing behavior due to increment in the values of  $P$ . Fig. 3 delineates the changings in temperature field due to accumulating thermophoresis parameter  $A$ . Temperature field presents increasing behavior due to rise in  $A$ . Fig. 4 points out on temperature distribution the corollary of Brownian motion parameter. The distribution of temperature goes up because of accelerating  $B$ . Fig. 5 displays the effects of modified Dufour parameter  $F$  on temperature distribution. An

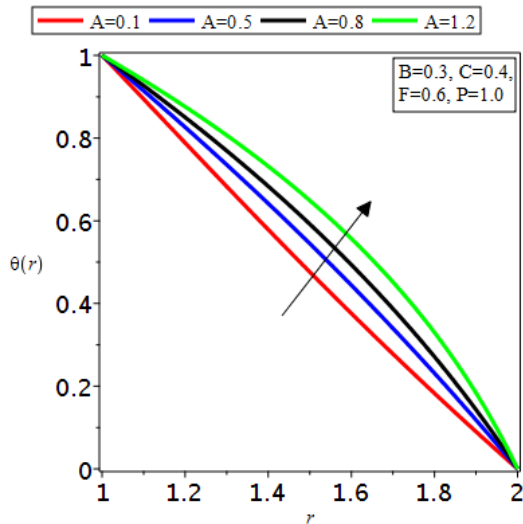


Figure 3: Effects of  $A$  on temperature distribution

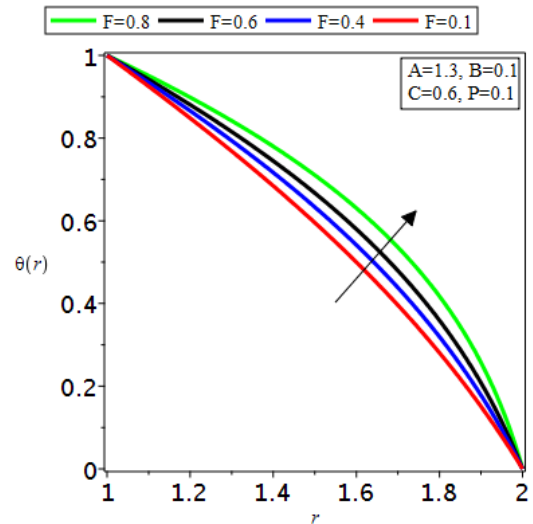


Figure 5: Influence of  $F$  on temperature profile

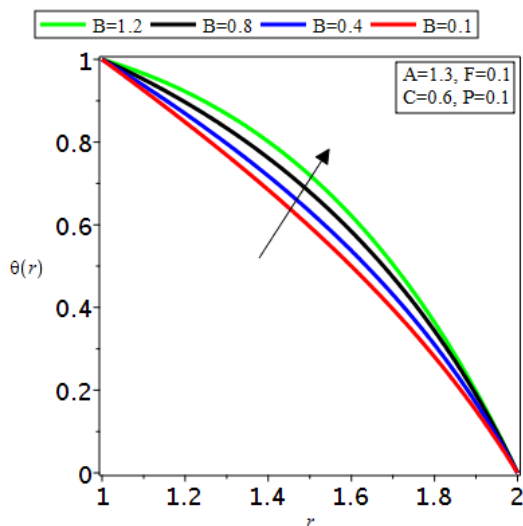


Figure 4: Influence of  $B$  upon Temperature field

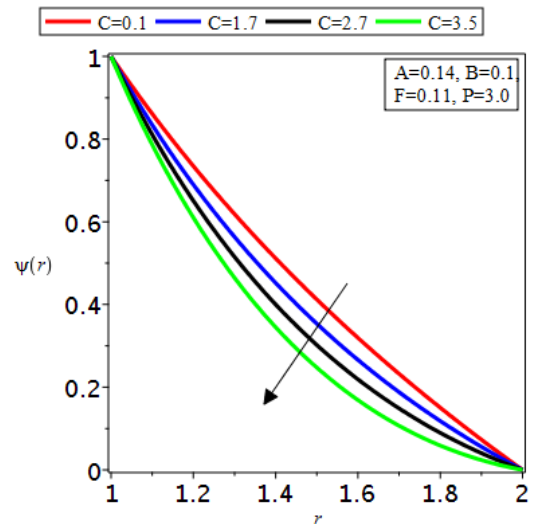


Figure 6: Effects of  $C$  on concentration profile

increase in pertinent parameter  $F$  causes increase in temperature distribution. Fig. 6 shows the influence of Dufour-solutal Lewis number  $C$  on concentration field. Fig. 7 explicates the influence of thermophoresis parameter on nano fraction profile. Physically increasing values of  $A$  shows the direct variation of parameter with nanoparticle fraction distribution. Fig. 8 explains the inverse effects of brownian motion parameter with nanoparticle profile. Fig. 9 depicts the effects of modified Dufour parameter  $F$  on nanoparticle fraction distribution. An increase in pertinent parameter  $F$  causes decrease in corresponding profile. For distinct values of  $A$ , figs. 10-12 demonstrate stream lines. Stream lines are going far from the origin due to intensifying values of  $A$ .

## 6. Conclusions

In prevailing investigation the effects of casso nanofluid flow between the two concentric cylinders are interpreted. Numerical results are obtained through governing equations. The obtained results satisfy the boundary conditions and the governing equations obviously. The impact of distinct parameters are also interpreted. Physically, an increasing value of thermophoresis parameter causes the enhancement of nanoparticle concentration. Some magnificent points of present investigation are summarized below:

1. The velocity field decreases due to the effect of increasing values of the casso parameter.
2. Due to having higher thermal conductivity, nanofluids are better coolants than their base fluid.
3. Temperature field represents inclination because of rise in Thermophoresis parameter and accumulating due to

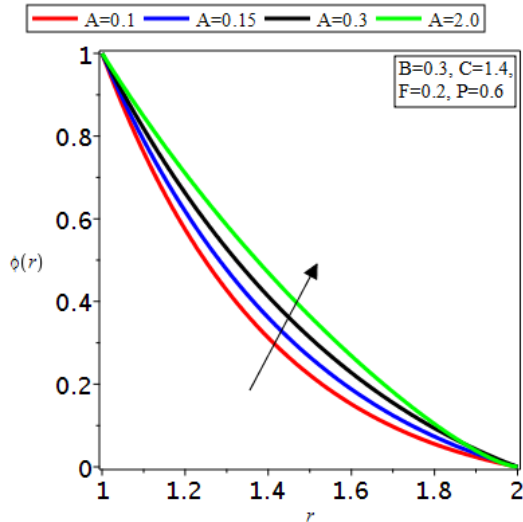


Figure 7: Nano particle fraction distribution for variation in  $A$

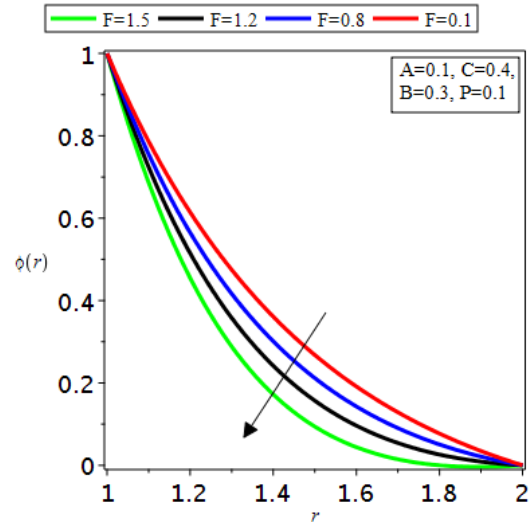


Figure 9: Nano particle fraction for variation in  $F$

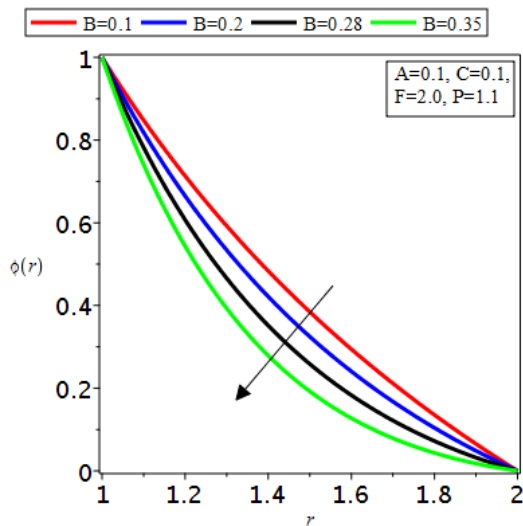


Figure 8: Nano particle fraction for variation in  $B$

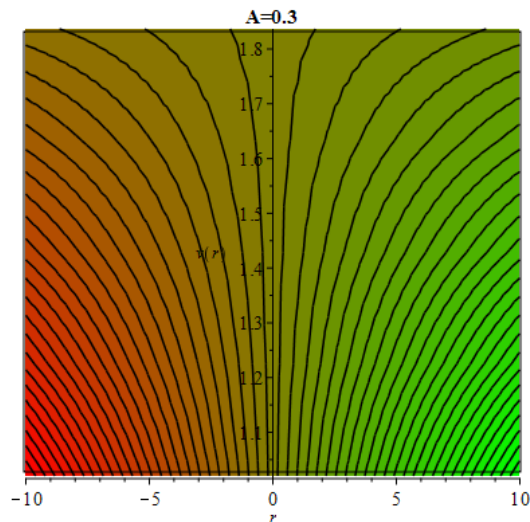


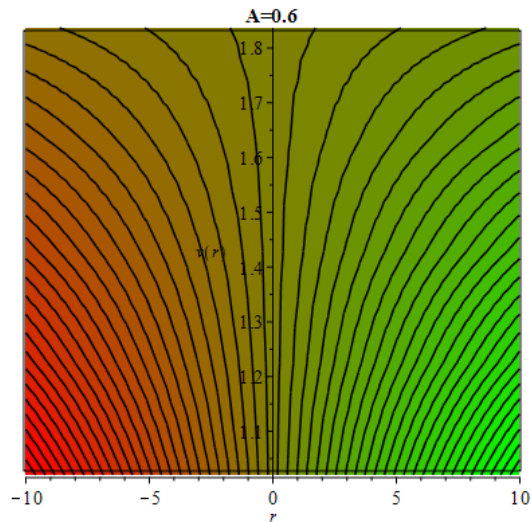
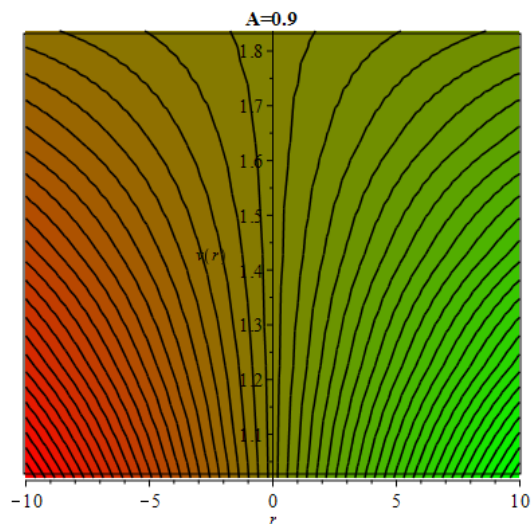
Figure 10: For  $A = 0.3$ , the behavior of Stream lines

acceleration in the values of Brownian motion parameter and Dufour-solutal lewis number.

4. Temperature gains a higher value than the mass fraction and nano particle concentration. The Dufour effects are inverse effects of thermophoresis. It is due to the addition of solid particle that causes the weaker molecular diffusivity which decays the concentration boundary layer thickness.
5. Stream lines illustrates the shrinking behavior when decreasing values for  $v(r)$ .

## References

- [1] M. Y. Malik, A. Hussain, S. Nadeem, T. Hayat, Flow of a third grade fluid between coaxial cylinders with variable viscosity, Zeitschrift für Naturforschung A 64 (9-10) (2009) 588–596.
- [2] D. Vieru, M. Nazar, C. Fetecau, C. Fetecau, New exact solutions corresponding to the first problem of stokes for oldroyd-b fluids, Computers & Mathematics with Applications 55 (8) (2008) 1644–1652.
- [3] W. Tan, T. Masuoka, Stokes' first problem for an oldroyd-b fluid in a porous half space, Physics of Fluids 17 (2) (2005) 023101.
- [4] M. Y. Malik, A. Hussain, S. Nadeem, Analytical treatment of an oldroyd 8-constant fluid between coaxial cylinders with variable viscosity, Communications in Theoretical Physics 56 (5) (2011) 933.
- [5] T. Hayat, S. Nadeem, A. M. Siddiqui, S. Asghar, An oscillating hydro-magnetic non-newtonian flow in a rotating system, Applied mathematics letters 17 (5) (2004) 609–614.
- [6] A. Shahzad, R. Ali, Approximate analytic solution for magneto-hydrodynamic flow of a non-newtonian fluid over a vertical stretching sheet, Can J Appl Sci 2 (1) (2012) 202–215.
- [7] M. Y. Malik, A. Hussain, S. Nadeem, Analytical treatment of an oldroyd 8-constant fluid between coaxial cylinders with variable viscosity, Communications in Theoretical Physics 56 (5) (2011) 933.
- [8] S. Nadeem, R. U. Haq, Z. Khan, Numerical solution of non-newtonian nanofluid flow over a stretching sheet, Applied Nanoscience 4 (5) (2014) 625–631.
- [9] M. Hameed, S. Nadeem, Unsteady mhd flow of a non-newtonian fluid

Figure 11: For  $A = 0.6$ , the behavior of Stream linesFigure 12: For  $A = 0.9$ , the behavior of Stream lines

on a porous plate, *Journal of Mathematical Analysis and Applications* 325 (1) (2007) 724–733.

- [10] M. Malik, I. Khan, A. Hussain, T. Salahuddin, Mixed convection flow of mhd eyring-powell nanofluid over a stretching sheet: A numerical study, *AIP advances* 5 (11) (2015) 117118.
- [11] R. U. Haq, S. Nadeem, Z. Khan, N. Noor, Mhd squeezed flow of water functionalized metallic nanoparticles over a sensor surface, *Physica E: Low-dimensional Systems and Nanostructures* 73 (2015) 45–53.
- [12] S. Nadeem, N. S. Akbar, Peristaltic flow of walter's b fluid in a uniform inclined tube, *Journal of Biorheology* 24 (1) (2010) 22–28.
- [13] M. Malik, M. Bibi, F. Khan, T. Salahuddin, Numerical solution of williamson fluid flow past a stretching cylinder and heat transfer with variable thermal conductivity and heat generation/absorption, *AIP Advances* 6 (3) (2016) 035101.
- [14] S. Nadeem, R. U. Haq, C. Lee, Mhd flow of a casson fluid over an exponentially shrinking sheet, *Scientia Iranica* 19 (6) (2012) 1550–1553.
- [15] A. Rehman, S. Achakzia, S. Nadeem, S. Iqbal, Stagnation point flow of eyring powell fluid in a vertical cylinder with heat transfer, *Journal of Power Technologies* 96 (1) (2016) 57–62.
- [16] M. Viloria Ochoa, Analysis of drilling fluid rheology and tool joint effect to reduce errors in hydraulics calculations, Ph.D. thesis, Texas A&M

University (2006).

- [17] R. Ellahi, Effects of the slip boundary condition on non-newtonian flows in a channel, *Communications in Nonlinear Science and Numerical Simulation* 14 (4) (2009) 1377–1384.
- [18] R. Ellahi, A. Riaz, Analytical solutions for mhd flow in a third-grade fluid with variable viscosity, *Mathematical and Computer Modelling* 52 (9–10) (2010) 1783–1793.
- [19] M. Sheikholeslami, D. D. Ganji, M. Y. Javed, R. Ellahi, Effect of thermal radiation on magnetohydrodynamics nanofluid flow and heat transfer by means of two phase model, *Journal of Magnetism and Magnetic Materials* 374 (2015) 36–43.
- [20] M. Sheikholeslami, M. G. Bandy, R. Ellahi, A. Zeeshan, Simulation of mhd cuo–water nanofluid flow and convective heat transfer considering lorentz forces, *Journal of Magnetism and Magnetic Materials* 369 (2014) 69–80.
- [21] M. Malik, I. Khan, A. Hussain, T. Salahuddin, Mixed convection flow of mhd eyring-powell nanofluid over a stretching sheet: A numerical study, *AIP advances* 5 (11) (2015) 117118.
- [22] R. U. Haq, S. Nadeem, Z. Khan, N. Noor, Mhd squeezed flow of water functionalized metallic nanoparticles over a sensor surface, *Physica E: Low-dimensional Systems and Nanostructures* 73 (2015) 45–53.